Engineering and Technology Journal
Journal homepage: https://etj.uotechnology.edu.iq

Evaluating land use land cover classification based on machine learning algorithms

Basheer S. Jasim [a,b] *, **Oday Z. Jasim** [b], **Amjed N. AL-Hameedawi** [b]

[a] Technical Institute of Babylon, Al-Furat Al-Awsat Technical University, Iraq
[b] Civil Engineering Dept., University of Technology-Iraq, Alsina'a street, 10066 Baghdad, Iraq.
*Corresponding author Email: basheer.jasim@atu.edu.iq

HIGHLIGHTS

- SVM, MD, and MLC were used to classify LULC in Babylon Governorate.
- SVM outperformed with 86.88% accuracy and a kappa of 0.83; MLC scored the lowest.
- SVM (14.20, 0.99, 49.08, 35.73)%, MD (24.58, 1.07, 35.58, 38.78)%, and MLC (22.87, 0.93, 35.27, 40.93)% for each class.

ARTICLE INFO

Handling editor: Imzahim A. Alwan

Keywords:
Machine Learning, LULC; Maximum Likelihood Classification; Mahalanobis Distance; Support Vector Machine.

ABSTRACT

Image classification depends substantially on the remote sensing method to generate maps of land use and land cover. This study used machine learning algorithms for classifying land cover, evaluating algorithms, and choosing the best way based on accuracy assessment matrices for land cover classifications. Satellite images from the Landsat by the United States Geological Survey (USGS) were used to classify the Babylon Governorate Land Use Land Cover (LULC). This study employed multispectral satellite images utilizing a spatial resolution of 30 meters and organized the data using three different algorithms to see the most accuracy. The process of categorization was carried out with the use of three distinct algorithms, which are as follows: Support Vector Machine (SVM), Mahalanobis Distance (MD), and Maximum Likelihood Classification (MLC). The classification algorithms utilized ArcGIS 10.8 and ENVI 5.3 software to detect four LULC classes: (Built-up Land, Water, Barren Land, and Agricultural Land). When applied to Landsat images, the results showed that the SVM approach gives greater overall accuracy and a larger kappa coefficient than the MD and MLC methods. SVM, MD, and MLC algorithms each have respective overall accuracy values of 86.88%, 85.00%, and 79.38%, respectively.

1. Introduction

Land Use Land Cover (LULC) is constantly changing with time at local, regional, and global scales [1,2]. Comprehending LULC changes is essential in many sectors that rely on Earth data, including factors like local and regional planning [3,4]. The accurate classification techniques are based on a sensor, spatial and spectral resolutions, and optical or active rolling environmental changes utilizing optical and microwave imaging from various sensors, and the approaches take into account ecological changes over time [5]. Land use research initiatives worldwide have been essential to international research on climate and environmental change [6]. The land topography and its subsequent uses can be monitored and planned more effectively with the assistance of LULC maps [7]. This cover may include water, vegetation, barren earth, and artificial structures [2]. In this respect, applying spectral classification to satellite images is of considerable use to planners and those concerned with the problem of the LULC [8,9].

Many different areas of research can benefit from high-resolution LULC classifications, the measurement of carbon storage, and the evaluation of environmental impact [10-13]. Monitoring the change in LULC has been identified as an essential component of a diverse range of activities and applications, including the planning for land use and minimizing the impacts of global warming [14,15]. Compared to alternative approaches, such as ground surveys, RS offers the chance for the speedy collection of information on LULC at a much lower cost [16,17]. Consequently, uncontrolled population growth and economic and industrial development, especially in new nations with higher LULC shifts, involve many human benefits [15],[18-20]. Recently, much interest has been in mapping LULC using machine-learning algorithms applied to remotely sensed imagery [21,22].

http://doi.org/10.30684/etj.2024.144585.1638
Received 12 November 2023; Received in revised form 28 January 2024; Accepted 02 February 2024; Available online 18 February 2024
2412-0758/University of Technology-Iraq, Baghdad, Iraq

The most crucial aspect in this research, vegetation, was taken into account along with evaporation temperature, land surface temperature, evapotranspiration, rainfall, snow cover, and soil moisture by Mokhtari and Akhoondzadeh. [23] using the Random Forest (RF), Decision Tree (DT), Support Vector Regression (SVR), and Artificial Neural Network (ANN) method, The Normalized Difference Vegetation Index (NDVI) is modeled and forecasted for monthly timescales. We could provide a model with the desired level of accuracy by using these techniques. The precision of the ANN technique is greater than that of the other three algorithms; moreover, an average accuracy with an RMSE of 0.0385.

Alwan and Aziz [24]. Satellite images with a spatial resolution of 10 meters were used, and three categorization algorithms were utilized to compare their accuracy using ENVI 5.1 software. The three main techniques used to complete the classification procedure were SVM, ANN, and MLC. Six land cover types were identified: barren soil, agricultural area, urban area (built-up region), marsh vegetation (aquatic vegetation), shallow water marsh, and deep-water marsh. The findings indicate that when employed in Sentinel 2B images, the MLC methodology provides greater overall accuracy and a higher kappa coefficient than the ANN and SVM techniques. The MLC algorithm had an overall accuracy of 85.32 percent, the ANN algorithm had a 70.64 percent overall accuracy, and the SVM algorithm had a 77.01 percent overall accuracy.

Using a map of forest cover categories as ground data, three different image categorization methods, ANN, SVM, and MLC, were used to classify GÜNLÜ satellite images [25]. Categorization technique outcomes were assessed depending on overall accuracies (OA) and kappa coefficients (KC). It was found that the OA varied from 76.82 to 96.67 percent, and the KC ranged from 0.66 to 0.95 once the categorization successes from the three classification techniques were analyzed. According to the findings, MLC had the greatest OA (ranging from 85.33% to 96.67%), followed closely by SVM (ranging from 80.11% to 91.93%), and then ANN (ranging from 76.82% to 89.92%).

Six ML algorithms, including Mahalanobis distance MD, Spectral Angle Mapper (SAM), fuzzy adaptive resonance theory-supervised predictive mapping, and spectral angle mapping (Fuzzy ARTMAP), ANN, SVM, and RF, are often utilized by Talukdar et al. [26] to evaluate the data. Index-based validation, the Receiver Operational Curve (RoC), the KC, and RMSE were used to measure accuracy. According to the KC findings, all classifications have an equivalent level of precision, with a few minor differences between them. Although the RF technique has the highest degree of precision (0.89), the MD method (parametric classification) has the lowest accuracy (0.82). According to this review's findings, the RF technique was the best for ML LULC classification among the six different algorithms evaluated.

Currently, numerous studies have been conducted on land-use classification using machine-learning algorithms. Still, the performance of models is not well examined for classifying past images with ancient history. Previous studies relied on Google Earth or Google Earth Engine (GEE) sites. This study will use high-resolution topographic maps to calculate classification accuracy. According to those mentioned above, the current research is carried out to identify and classifier evaluate the land cover in Babylon Governorate in Iraq in the year 2002 by using remote sensing datasets and GIS analysis to be used in the study of the region by performing detailed analyses.

The main objective of this study employed RS and GIS techniques to classify and map the LULC of the studied area. This article uses three machine-learning techniques that can produce a high-precision LULC map. In addition, an accuracy assessment is performed to interpret the best classification algorithm.

2. Material and method

Because there has been a substantial amount of study conducted in the field of image processing using machine learning, it is possible to accomplish this goal by utilizing approaches associated with machine learning. A considerable variety of supervised machine-learning algorithms can carry out image-processing tasks. These algorithms are based on the concept of machine learning.

2.1 Dataset

This study used the Landsat 5 Thematic Mapper image for the year 2002 to plot the LULC using three different machine-learning algorithms. The image was obtained by downloading it from the USGS. After an exhaustive review of the relevant prior research and discussion with subject matter specialists, the researcher determined four first-order LULC classes. Table 1. shows that the images have a resolution of 30 meters and no clouds. Before the geo-special analysis, the images were radiometrically and the atmosphere by radiometric calibration and atmospheric correction. Table 1 illustrates the satellite data acquisition.

Table 1: Satellite information was used for this study

No.	Satellite	Sensor	Path/Row	Date of acquisition	Resolution	Product type	Cloud cover
1	Landsat 5	TM	168/38	22/10/2002	30 m	Landsat Collection 1 Level-1	0%
2	Landsat 5	TM	168/37	22/10/2002			

2.2 Study area

Babylon Governorate may be considered to be in the geographic middle of Iraq, located around 100 km to the south of Baghdad, the capital of Iraq, between the longitudes of 44º2'43" East and 45º12'11" East, as well as the latitudes of 32º5'41" North and 33º7'36" North. Administratively, five major cities make up the Governorate as a whole. These significant cities

include Al-Hillah, Al-Qasim, Al-Hashimiyah, Al-Mahawil, and Al-Musayiab. According to calculations made using the program ArcGIS 10.8, the research region covers an area of about 5338 km^2. Figure 1 shows the study area map.

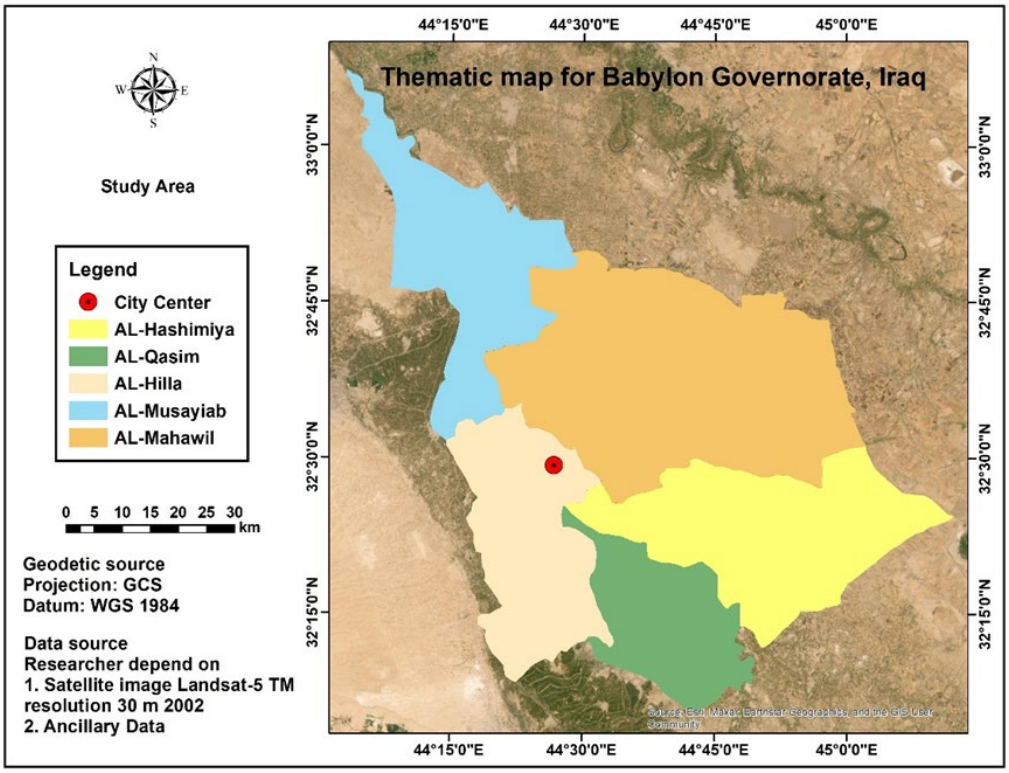

Figure 1: Geographical location map of Babylon Governorate

2.3 Supervised land cover classification

The first step in supervised classification is identifying the regions used as simulated training locations for the various land cover classifications [5]. A method known as supervised classification is one in which the user works as a supervisor for pixel categorization. Extracting classes from a satellite image containing multispectral bands is carried out if a pixel being investigated matches a specific statical situation. Therefore, this image is classified accordingly [27]. The amount of experience the analyzer possesses is a significant factor that determines the image classification results by explaining the land cover spectrum signature. After that, the computer software utilizes the spectral properties of this training section to classify the whole image [28]. Classification is the primary method for extracting information about different types of land cover from RS images. In the context of the study of RS, classification refers to transforming data into land cover classifications with specific biogeophysical functions [29].

The word land use relates to the activities carried out by humanity in a specific place and at a particular point in time [30]. Land use in any community is a reflection of the economic and social growth of the country. Land use is of utmost significance in many nations because it guides the country's potential for economic and social development [31]. The change detection process requires using many temporal datasets to quantitatively analyze the phenomenon's impacts on the period [32,33]. Monitoring local, regional, and global resources and environments requires information on changes that occur on the earth's surface [34,35]. The most necessary primary material for constructing geographic libraries in general, but in particular when it involves utilizing raster data [36]. In machine learning, the choice of method is determined by factors such as sample size, the number of samples taken, the variable being trained on, and the total amount of training data [37,38]. The most widely used machine-learning classifiers were used throughout the LULC classification process. The analysis of LULC is carried out using the following software: (ArcGIS 10.8 and ENVI 5.3). Methods for Machine-Learning Classifiers:

2.3.1 Support vector machine

The Support Vector Machine (SVM), which was developed by Vapnik in 1995, is a technique for supervised learning algorithms [39,40]. The support vector machine is one of the most successful techniques for classification. It is a machine-learning method that can potentially enhance class boundary lines [28]. The model is based on a user-defined kernel function, and it is put to use in transferring nonlinear decision boundaries found in a dataset to the linear limits of a high-dimensional construct [41]. The formula used to find a support vector machine is illustrated in Equation 1 [41]:

$$g(x) = sign\left(\sum_{i=1}^{n} 1^{y_i}\ \alpha_j\ K\left(x_i, x_j\right) + b\right) \quad (1)$$

where:
$K(x_i, x_j)$ is the kernel function.
αj is the Lagrange multiplier for the inequality constraint.
yi is an indicator of the state of the company.
b is a constant.

2.3.2 Mahalanobis distance

Estimating the correlation matrix for each class is required to assign a test image to one of the N numbers of classes. First, it determines a classification according to the minimum Euclidean distance, and then it considers the direction sensitivity according to the covariance matrix [27]. A lower value for MD indicates a greater likelihood that an observation will be nearer to the group center. The MD (D_k^2) towards class averages is computed according to the following expression for each feature vector illustrated in Equation 2 [42]:

$$D_k^2 = (x_i - \bar{x}_k)^T \, S_K^{-1} (x_i - \bar{x}_k) \quad (2)$$

where x_i is the vector that represents the pixel of image data, $\bar{x}_k$ is the sample mean vector of the k[th] class, S_K^{-1} represents the variance and covariance matrix for class i; and T defines a transposition of the matrix.

2.3.3 Maximum likelihood classification

MLC is the image classification method utilized most often in practice [27]. It is predicated on the hypothesis that the training data statistics in each band are distributed in a typical way. In addition to this, it computes the variance-covariance matrix for each class based on the distances toward the category means [5]. The Bayesian probability formula is the basis for MLC methodology [43]. The formula used to find Maximum likelihood is illustrated in Equation 3 [43] :

$$P(x, w) = P\left(\frac{w}{x}\right) P(x) = P\left(\frac{x}{w}\right) P(w) \quad (3)$$

where x and w refer to the events, P(x,w) is the likelihood that events might happen together, P(x) and P(w) is the probability that existed before an event occurred, and P(w/x) is the probability of event x given the presence w.

2.3.4 Classification accuracy assessment

Validation of the accuracy of the obtained categorized images using a kappa index and an error matrix [44]. The formula was calculated using the kappa coefficient, which Congalton and Green also used to corroborate and validate their findings [45]. The formula used to find kappa coefficients is illustrated in Equation 4 [45]:

$$\text{Kappa coefficient} = \frac{\sum_{i=1}^{k} n_{ii} - \sum_{i=1}^{k} n_{ii}(G_i C_i)}{n^2 - \sum_{i=1}^{k} n_{ii}\,(G_i C_i)} \quad (4)$$

Where i is the number of the class, n is the total number of pixels that have been classified and will be compared with the actual data, nii represents the number of pixels that are part of the introductory data class i, that were classified as belonging to class i, Ci is the total number of pixels that correspond to class i that have been organized. Gi represents the total number of actual data pixels that belong to class i.

It is regarded as having weak judgment when the kappa coefficient value is less than 0.20 (<0.2). The value from 0.20 to 0.40 is in the middling range, while the value from 0.4 to 0.6 has a reasonable consensus. In conclusion, an accuracy of extremely excellent agreement between the LULC classification and actual ground data may be found between 0.8 and 1 [7],[46].

The overall classification accuracy guides the percentage of cells that have been accurately categorized; it is the most common measure used because it is simple to understand and has significant significance in reality [47]. The formula used to find overall classification accuracy is illustrated in Equation 5 [13]:

$$\text{Overall accuracy} = \frac{\text{Number of correct classes}}{\text{Total number of classes}} \quad (5)$$

3. Methodology

The study will use the theory method of LULC mapping of Babylon Governorate based on Geomatics techniques and the practical approach used in this paper, which can be illustrated and described as follows:

1) Data collection from a satellite.
2) Data processing (Composite Bands, Mosaic Image, Radiometric Calibration, Atmospheric Correction, Subset).
3) Apply three classification algorithms, SVM, MD, and MLC, utilizing ArcGIS 10.8 and ENVI 5.3 software to extract different LULC classes (Built-up Land, Water, Barren Land, and Agricultural Land).
4) Extracting LULC.

Assess the accuracy and compare the results. Figure 2 illustrates the methodology flowchart, and Table 2. describes class information.

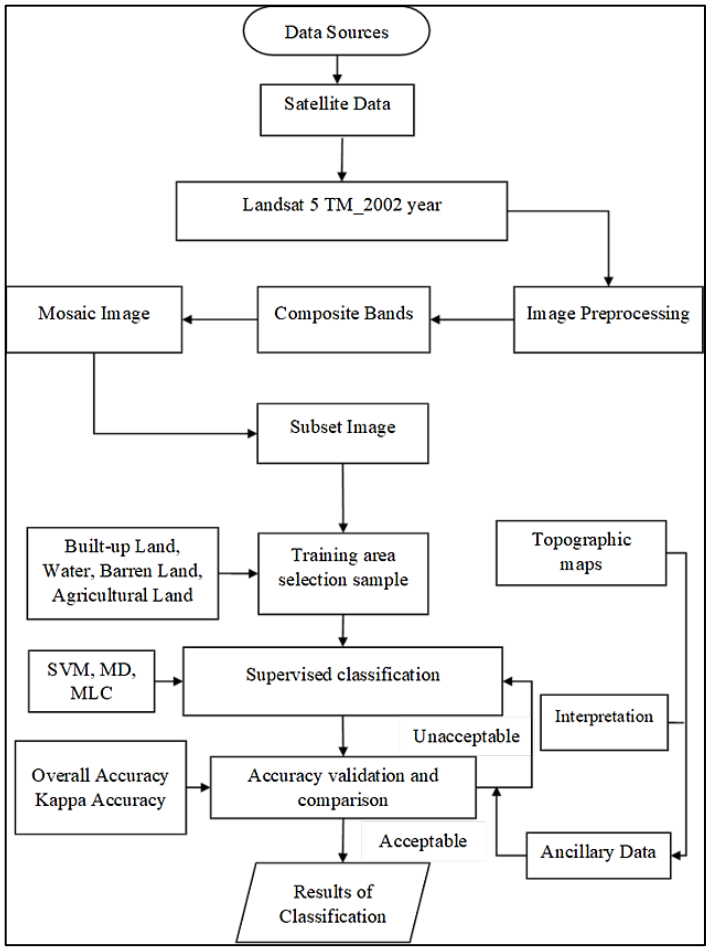

Figure 2: The methodology steps to perform the classification

Table 2: LULC classification classes of Babylon Governorate

No.	Classes	Description
1	Barren Land	Soil surface, salty lands, rocky and sandy fields.
2	Built-up Land	Urban and rural residential areas, industrial and commercial buildings, roads, and transportation facilities.
3	Agricultural Land	Agricultural and garden lands, grass and bush pastures, city parks.
4	Water	Lakes, rivers, canals.

4. Results and discussion

4.1 Comparison between classification

After collecting the signature and the reference samples, classification was carried out. The remote sensing image processing software ArcGIS 10.8 and ENVI 5.3 were used to carry out the three classification techniques: SVM, MD, and MLC. Four land cover classes were distinguished (Barren Land, Built-up Land, Agricultural Land, and Water), as shown in Figures 3 to 5. After that, the area and proportion for each class were determined, and the results are presented in Table 3. The broad classification was used since the primary concern of this investigation is the precision of classification systems in general. In addition, excellent detailed categorization calls for more detailed field data, which is difficult and expensive to collect in the research region. Compared to the MLC and SVM classification techniques, the MD classification method offers a more significant percentage of land to the Built-up Land class category. In contrast, the MLC and MD classification techniques provide smaller area percentages for the Barren Land, and the SVM classification method produces a more extensive area for the Barren Land. Consequently, the MD and SVM classification algorithms were more sensitive to the Built-up Land class and the Barren Land. Comparable with many researchers such as [24],[1] and [26].

Compared to the SVM and MD classification techniques, the findings of the MLC classification method indicate a lower area percentage in the Water class. However, the amount of land covered by vegetation differs significantly throughout the three

categorization techniques. Comparable with many researchers such as [23], [25]. Furthermore, not all machine-learning techniques produce a high-precision LULC map because good results depend on the machine-learning model set-up, training samples, and input parameters.

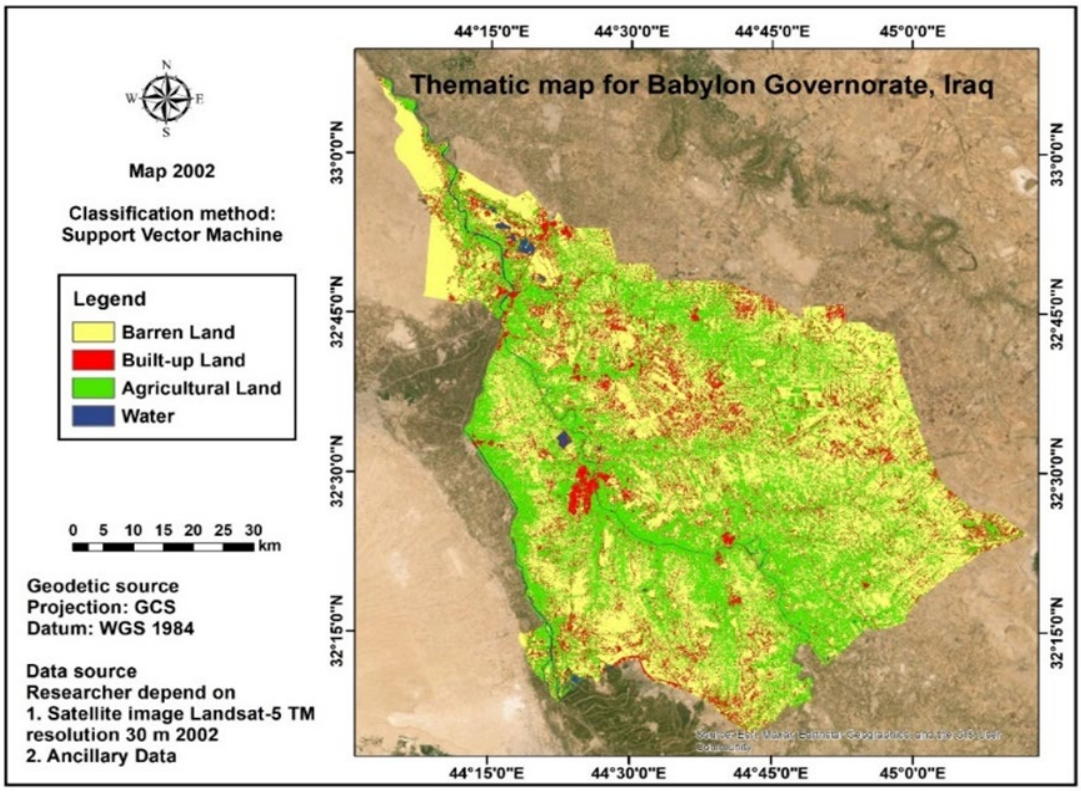

Figure 3: Classification by the algorithm of SVM

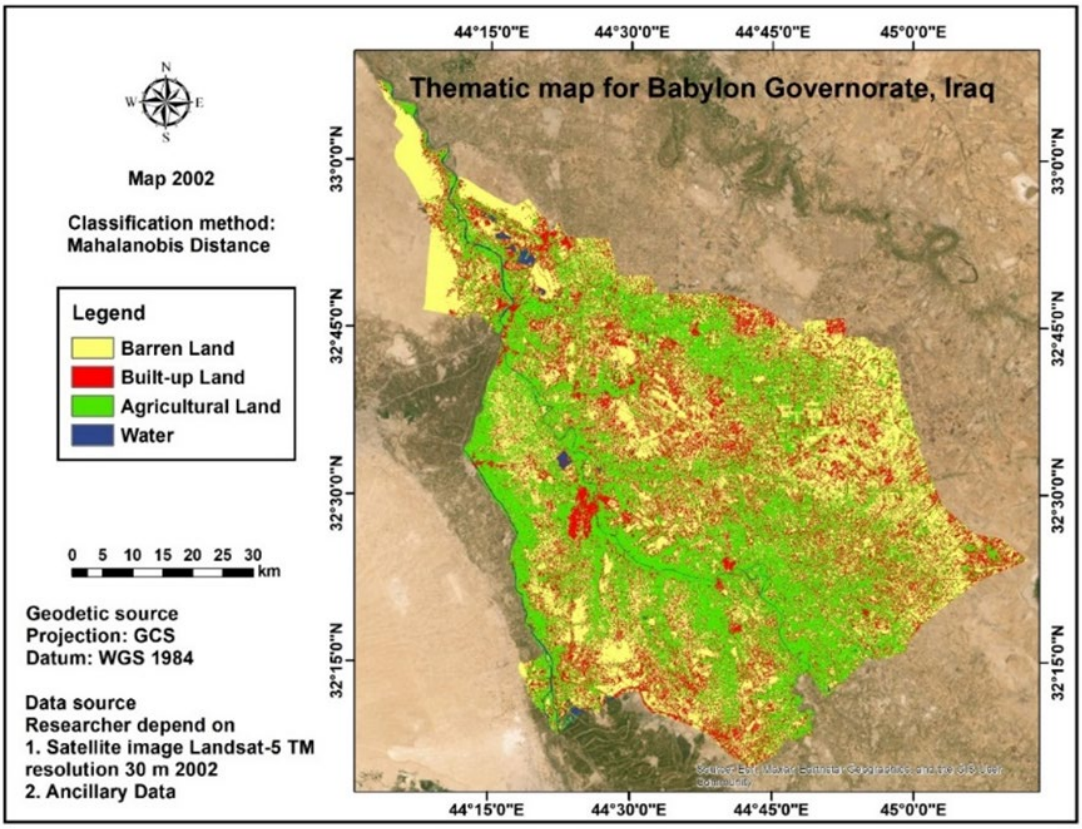

Figure 4: Classification by the algorithm of MD

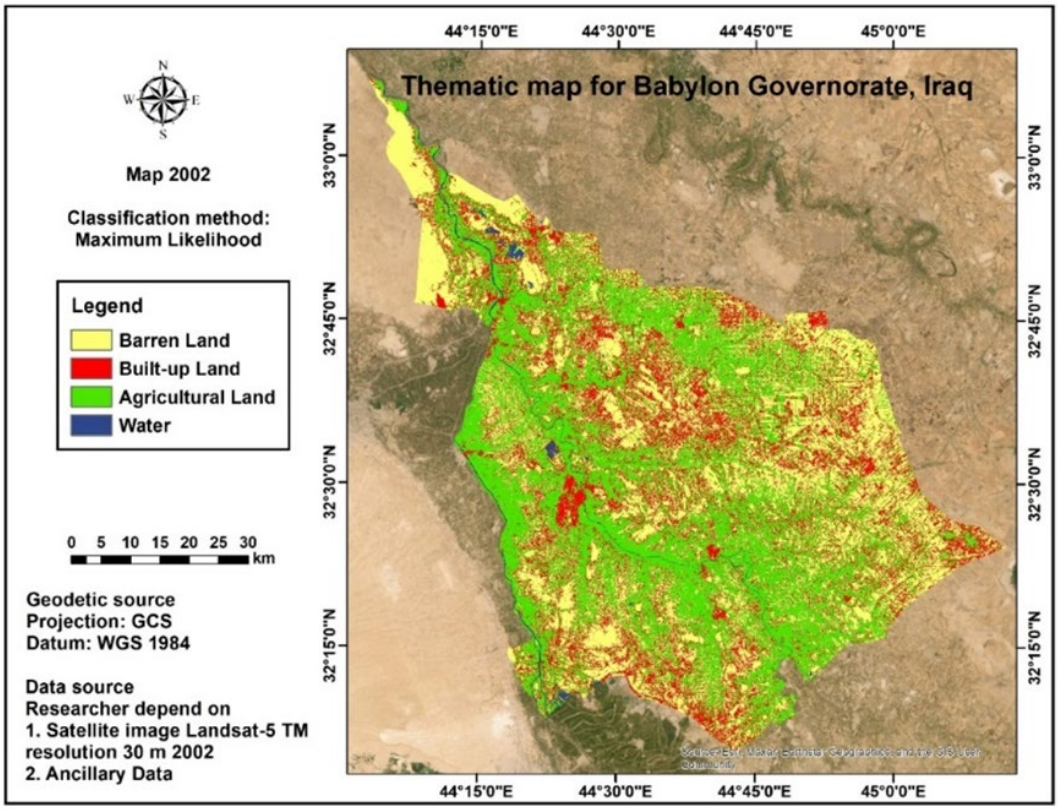

Figure 5: Classification by the algorithm of MLC

Table 3: Area and percentage for each class

Classes	SVM Percentage (%)	SVM Area (km²)	MD Percentage (%)	MD Area (km²)	MLC Percentage (%)	MLC Area (km²)
Built-up Land	14.20	757.62	24.58	1311.60	22.87	1220.74
Water	0.99	53.05	1.07	57.00	0.93	49.46
Barren Land	49.08	2619.27	35.58	1898.82	35.27	1882.16
Agricultural Land	35.73	1907.11	38.78	2069.63	40.93	2184.70
Total	100.00	5337.05	100	5337.05	100	5337.06

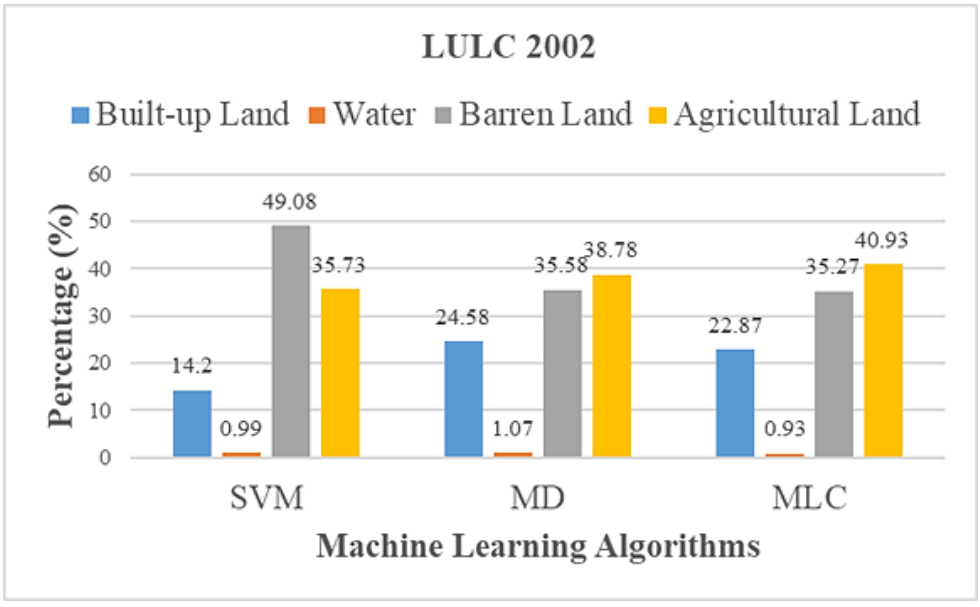

Figure 6: Comparison results of SVM, MD, and MLC

Before assessing the three algorithms used, the present study draws attention to the fact that the results of the percentage of built-up land and barren land are substantially different in the SVM classification compared to MD and MLC. However, the Water and Agricultural Land percentage results are close to a certain extent between the algorithms. These variations were seen in most of the studies performed by previous researchers. As a result, most of the suggestions were that many algorithms should be evaluated to determine the most suitable for the research field in each future work. In addition, it should be mentioned that the percentage of Barren Land computed in the SVM algorithm was far greater than that of Agricultural Land. Whereas the percentage of Agricultural Land was significantly lower in the MD and MLC algorithms, it was slightly higher than that of Barren Land. It is essential to mention that the training samples were similar for all the different algorithms utilized. Figure 6 presents all of the data for classification, organized according to the three methods.

4.2 Accuracy of methods

The first stage in determining the accuracy of a measurement is collecting the reference data, which consists of approximately 160 points divided into 40 points for each class created based on ancillary data such as topographic maps, as in Figure 7. These points were chosen from many places, each representing a particular land cover class. A cross-tabulation matrix was used to validate the collected findings by comparing the data of the classed images with those of the reference samples. The following items were obtained: the kappa index, which displays the degree of similarity between a set of control fields and the image that has been categorized; the overall accuracy, which indicates the proportion of pixels that have been correctly identified.

Table 4 presents the results that can be gained from applying the cross-tabulation matrix to verify the classified images, which includes the characteristics of this validation process, including general accuracy and kappa coefficient. Compared with the MD and MLC classification methods, the SVM classification method had an average accuracy of 86.88% and a kappa value of 0.83. In contrast, the overall accuracy of the MD classification method was 85% with a kappa value of 0.8, and the overall accuracy of the MLC classification method was 79.38% with a kappa value of 0.73. The MLC classification method was the least true of the three classification methods. The results from the SVM technique using Landsat data had the most fantastic accuracy out of the three major categorization algorithms.

Figure 8 shows the number of points selected for algorithm assessment using auxiliary data to the SVM, MD, and MLC methods. The overall number of valid attributes for all classes of data was (139 of 160), (136 of 160), and (127 of 160) points, respectively.

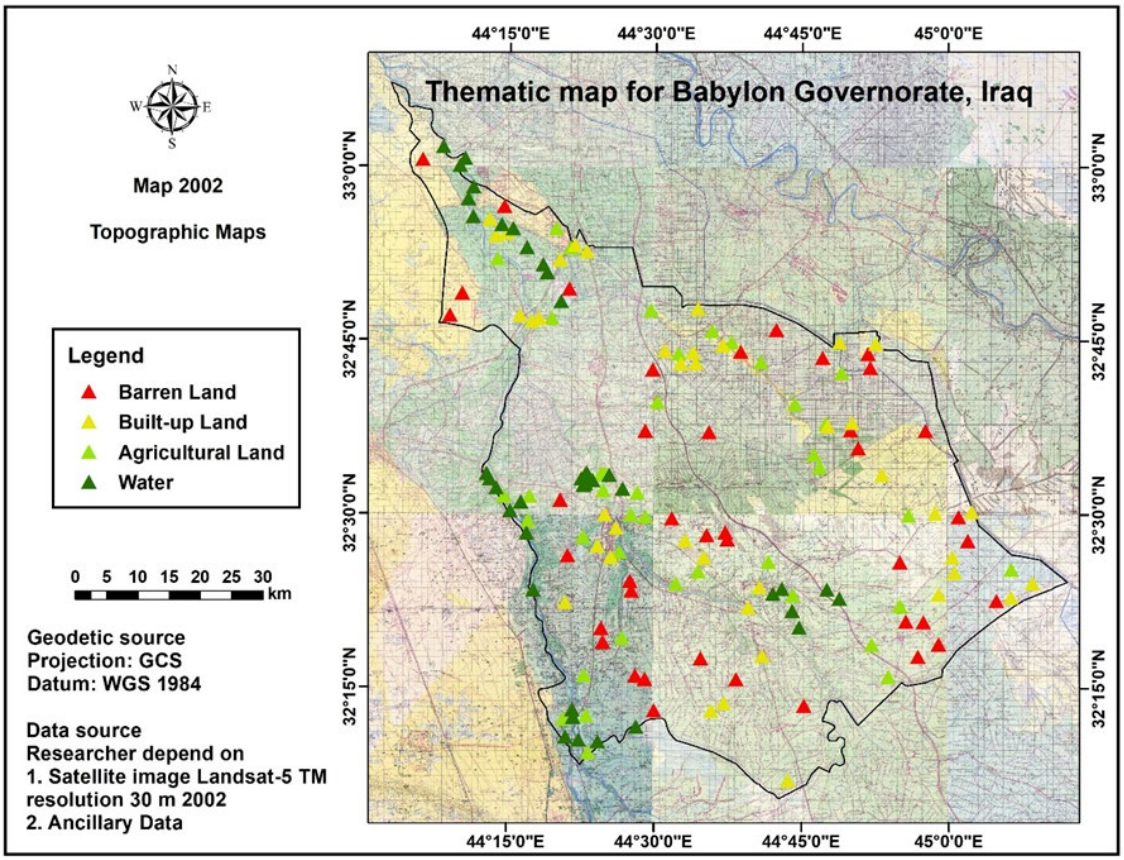

Figure 7: Reference data for each class

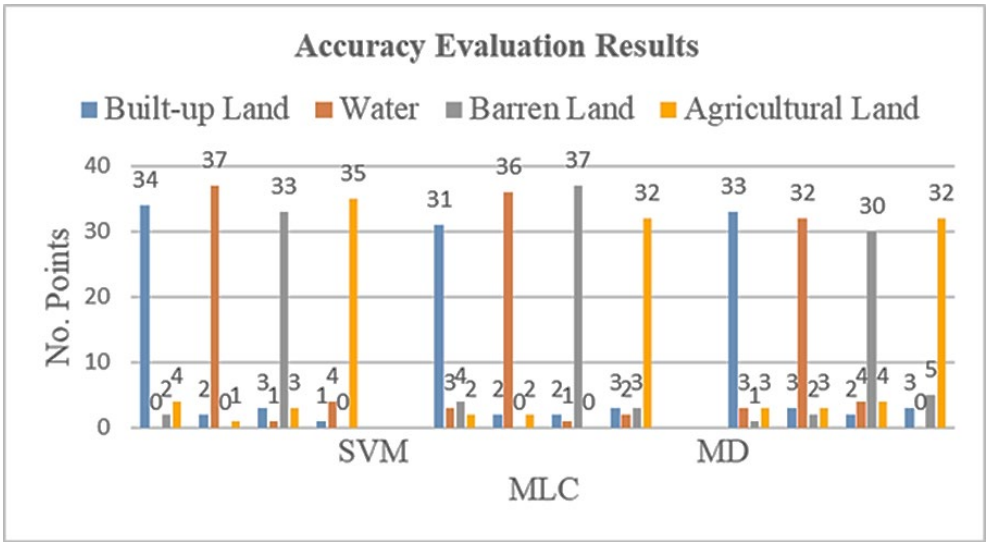

Figure 8: Illustrates the evaluation accuracy

Table 4: Accuracy evaluation results for SVM, MD, and MLC classification methods

Classifiers	Classes	Built-up Land	Water	Barren Land	Agricultural Land	Total	Overall Accuracy %	Kappa Coefficient
SVM	Built-up Land	34	2	3	1	40	86.88	0.83
	Water	0	37	1	4	42		
	Barren Land	2	0	33	0	35		
	Agricultural Land	4	1	3	35	43		
	Total	40	40	40	40	160		
Class accuracy %		85	92.5	82.5	87.5			
MD	Built-up Land	31	2	2	3	38	85.00	0.80
	Water	3	36	1	2	42		
	Barren Land	4	0	37	3	44		
	Agricultural Land	2	2	0	32	36		
	Total	40	40	40	40	160		
Class accuracy %		77.5	90	92.5	80			
MLC	Built-up Land	33	3	2	3	41	79.38	0.73
	Water	3	32	4	0	39		
	Barren Land	1	2	30	5	38		
	Agricultural Land	3	3	4	32	42		
	Total	40	40	40	40	160		
Class accuracy %		82.5	80	75	80			

5. Conclusion

Image classification is a procedure that may be used to produce LULC maps, which is one of many applicable remote sensing uses. This work evaluates the accuracy of three machine learning classifiers used for LULC mapping based on satellite data. According to the results:

1) Comparing the accuracy using land sat -5 TM, overall accuracy values for SVM, MD, and MLC methods were 86.88%, 85.00%, and 79.38%, respectively.
2) The area covered by each LULC class appears to vary depending on the classification method used in SVM (14.20, 0.99, 49.08, 35.73) %, MD (24.58, 1.07, 35.58, 38.78)%, and MLC (22.87, 0.93, 35.27, 40.93) %, according to (Built-up Land, Water, Barren Land, and Agricultural Land), respectively.
3) The kappa coefficient and index-based analysis indicate that the support vector machine (SVM) has the most fantastic accuracy of all the classifiers used in this investigation. Depending on its value, the overall accuracy is 86.88, and the kappa coefficient is 0.83%, as in Table 4.
4) Existing research on the topic was reviewed, and most studies concluded that SVM or MLC is the most effective classifier.

5) Furthermore, many studies concluded that the accuracy of LULC mapping shifts depending on the period and the location.
6) Three machine-learning techniques were used to classify the LULC data obtained from Landsat 5 TM. The Kappa coefficient, an index-based approach, was used with empirical data to evaluate accurately. The high accuracy evaluation for SVM for Water and low accuracy evaluation for Barren Land are shown in Figure 7.

Therefore, as a suggestion for further research, it is advised to investigate the accuracy of the classifiers under various meteorological situations.

Author contributions

Conceptualization, B. Jasim. And O. Jasim; methodology, A. AL-Hameedawi.; software, B. Jasim.; validation, B. Jasim., O. Jasim. and A. AL-Hameedawi.; formal analysis, B. Jasim.; investigation, O. Jasim.; resources, B. Jasim.; data curation, A. AL-Hameedawi.; writing—original draft preparation, A. AL-Hameedawi.; writing—review and editing, A. AL-Hameedawi.; visualization, B. Jasim.; supervision, O. Jasim.; project administration, O. Jasim.; All authors have read and agreed to the published version of the manuscript.

Funding

This research received no specific grant from any funding agency in the public, commercial, or not-for-profit sectors.

Data availability statement

The data supporting this study's findings are available on request from the corresponding author.

Conflicts of interest

The authors declare that there is no conflict of interest.

References

[1] O. Z. Jasim, Using of machines learning in extraction of urban roads from DEM of LIDAR data: Case study at Baghdad expressways, Iraq, Period. Eng. Nat. Sci., 7 (2019) 1710–1721. http://dx.doi.org/10.21533/pen.v7i4.914

[2] O. Jasim, K. Hasoon, and N. Sadiqe, Mapping LCLU Using Python Scripting, Eng. Technol. J., 37 (2019) 140–147. https://doi.org/10.30684/etj.37.4A.5

[3] N. Hashem and P. Balakrishnan, Change analysis of land use/land cover and modelling urban growth in Greater Doha, Qatar, Ann. GIS, 21 (2015) 233–247. https://doi.org/10.1080/19475683.2014.992369

[4] A. Rahman, S. Kumar, S. Fazal, and M. A. Siddiqui, Assessment of land use/land cover change in the North-West District of Delhi using remote sensing and GIS techniques, J. Indian Soc. Remote Sens., 40 (2012) 689–697. http://dx.doi.org/10.1007/s12524-011-0165-4

[5] O. O. Omo-Irabor, A comparative study of image classification algorithms for landscape assessment of the Niger Delta Region, J. Geogr. Inf. Syst., 8 (2016) 163–170. http://dx.doi.org/10.4236/jgis.2016.82015

[6] H. Han, C. Yang, and J. Song, Scenario simulation and the prediction of land use and land cover change in Beijing, China, Sustainability, 7 (2015) 4260–4279. https://doi.org/10.3390/su7044260

[7] N. Ya'Acob, I. A. A. Jamil, N. F. A. Aziz, A. L. Yusof, M. Kassim, and N. F. Naim, Hotspots Forest Fire Susceptibility Mapping for Land Use or Land Cover using Remote Sensing and Geographical Information Systems (GIS), IOP Conf. Ser. Earth Environ. Sci., 1064 (2022). https://doi.org/10.1088/1755-1315/1064/1/012029

[8] M. H. Al-Helaly, I. A. Alwan, and A. N. Al-Hameedawi, Land covers monitoring for Bahar-Al-Najaf (Iraq) based on sentinel-2 imagery, J. Phys. Conf. Ser., 1973 (2021) 012189. https://doi.org/10.1088/1742-6596/1973/1/012189

[9] Z. M. Kadhum, B. S. Jasim, and A. S. J. Al-saedi, Improving the spectral and spatial resolution of satellite image using geomatics techniques Improving the Spectral and Spatial Resolution of Satellite Image Using Geomatics Techniques, 2776 (2023) 040011. https://doi.org/10.1063/5.0138463

[10] A. R. T. Ziboon, I. A. Alwan, and A. G. Khalaf, Utilization of remote sensing data and GIS applications for determination of the land cover change in Karbala Governorate, Eng. Technol. J., 31 (2013) 2773-2787. https://doi.org/10.30684/etj.31.15A.1

[11] E. Głowienka and K. Michałowska, Analyzing the Impact of Simulated Multispectral Images on Water Classification Accuracy by Means of Spectral Characteristics, Geomatics Environ. Eng., 14 (2020) 47–58. https://orcid.org/0000-0001-7326-1592

[12] Z. E. Hussein, R. H. Hasan, and N. A. Aziz, Detecting the changes of AL-Hawizeh Marshland and surrounding areas using GIS and remote sensing techniques, Assoc. Arab Univ. J. Eng. Sci., 25 (2018) 53–63. https://jaaru.org/index.php/auisseng/article/view/109

[13] I. A. Alwan, N. A. Aziz, and M. N. Hamoodi, Potential water harvesting sites identification using spatial multi-criteria evaluation in Maysan Province, Iraq, ISPRS Int. J. Geo-Information, 9 (2020) 235. https://doi.org/10.3390/ijgi9040235

[14] S. Reis, Analyzing land use/land cover changes using remote sensing and GIS in Rize, North-East Turkey, Sensors, 8 (2008) 6188–6202. https://doi.org/10.3390/s8106188

[15] D. Dutta, A. Rahman, S. K. Paul, and A. Kundu, Changing pattern of urban landscape and its effect on land surface temperature in and around Delhi, Environ. Monit. Assess., 191 (2019) 1-15. https://doi.org/10.1007/s10661-019-7645-3

[16] Z. Chen and J. Wang, Land use and land cover change detection using satellite remote sensing techniques in the mountainous Three Gorges Area, China, Int. J. Remote Sens., 31 (2010) 1519–1542. http://dx.doi.org/10.1080/01431160903475381

[17] M. Pal and P. M. Mather, Assessment of the effectiveness of support vector machines for hyperspectral data, Futur. Gener. Comput. Syst., 20 (2004) 1215–1225. https://doi.org/10.1016/j.future.2003.11.011

[18] N. Thanh Hoan et al., Assessing the effects of land-use types in surface urban heat islands for developing comfortable living in Hanoi City, Remote Sens., 10 (2018) 1965. https://doi.org/10.3390/rs10121965

[19] A. Rahman, S. P. Aggarwal, M. Netzband, and S. Fazal, Monitoring urban sprawl using remote sensing and GIS techniques of a fast growing urban centre, India, IEEE J. Sel. Top. Appl. earth Obs. Remote Sens., 4 (2010) 56–64. https://doi.org/10.1109/JSTARS.2010.2084072

[20] B. Kumari, M. Tayyab, H. T. Hang, M. F. Khan, and A. Rahman, Assessment of public open spaces (POS) and landscape quality based on per capita POS index in Delhi, India, SN Appl. Sci., 1 (2019) 1–13. https://doi.org/10.1007/s42452-019-0372-0

[21] A. E. Maxwell, T. A. Warner, and F. Fang, Implementation of machine-learning classification in remote sensing: An applied review, Int. J. Remote Sens., 39 (2018) 2784–2817. https://doi.org/10.1080/01431161.2018.1433343

[22] E. Adam, O. Mutanga, J. Odindi, and E. M. Abdel-Rahman, Land-use/cover classification in a heterogeneous coastal landscape using RapidEye imagery: evaluating the performance of random forest and support vector machines classifiers, Int. J. Remote Sens., 35 (2014) 3440–3458. https://doi.org/10.1080/01431161.2014.903435

[23] R. Mokhtari and M. Akhoondzadeh, Data fusion and machine learning algorithms for drought forecasting using satellite data, J. Earth Sp. Phys., 46 (2020) 231–246. https://doi.org/10.22059/jesphys.2020.299445.1007199

[24] I. A. Alwan and N. A. Aziz, An accuracy analysis comparison of supervised classification methods for mapping land cover using sentinel 2 images in the al-hawizeh marsh area, southern iraq, Geomatics Environ. Eng., 15 (2021) 5–21. http://dx.doi.org/10.7494/geom.2021.15.1.5

[25] A. GÜNLÜ, Multispektral ve Birleştirilmiş Uydu Görüntüleri Kullanılarak Arazi Örtüsü Sınıflandırılmasında Farklı Sınıflandırma Yaklaşımlarının Karşılaştırılması: Ören Orman İşletme Şefliği Örneği, Bartın Orman Fakültesi Derg., 23 (2021) 1–1. http://dx.doi.org/10.24011/barofd.882471

[26] S. W. Wang, B. M. Gebru, M. Lamchin, R. B. Kayastha, and W. K. Lee, Land use and land cover change detection and prediction in the kathmandu district of nepal using remote sensing and GIS, Sustain., 12 (2020) 3925. https://doi.org/10.3390/su12093925

[27] A. Ahmed, M. Muaz, M. Ali, M. Yasir, S. Ullah, and S. Khan, Mahalanobis distance and maximum likelihood based classification for identifying tobacco in Pakistan, in 2015 7th International Conference on Recent Advances in Space Technologies,RAST (2015) 255–260. http://dx.doi.org/10.1109/RAST.2015.7208351

[28] K. O. Murtaza and S. A. Romshoo, Determining the suitability and accuracy of various statistical algorithms for satellite data classification, Int. J. geomatics Geosci., 4 (2014) 585–599.

[29] D. P. Zourarakis, Remote Sensing Handbook–Volume I: Remotely Sensed Data Characterization, Classification, and Accuracies, Photogramm. Eng. Remote Sens., 84 (2018) 481. https://doi.org/10.14358/PERS.84.8.481

[30] H. Husein, O. Jasim, and S. Mahmood, Proposal of building a standard geodatabase for urban land use, MATEC Web Conf., 162 (2018) 1–5. https://doi.org/10.1051/matecconf/201816203024

[31] R. Al-Anbari, Oday Zakariya, and Z. T. Mohammed, Environmental and Urban Land Use Analysis by GIS in AL-Shaab of Baghdad as a case study, Eng. Technol. J., 34 (2016) 2272-2281. https://doi.org/10.30684/etj.34.12A.10

[32] Z. M. Kadhum, B. S. Jasim, and M. K. Obaid, Change detection in city of Hilla during period of 2007-2015 using Remote Sensing Techniques, IOP Conf. Ser. Mater. Sci. Eng., 737 (2020) 012228. https://doi.org/10.1088/1757-899X/737/1/012228

[33] B. S. Jasim, Z. M. K. Al-Bayati, and M. K. Obaid, Accuracy of horizontal coordinates of cadastral maps after geographic regression and their modernization using gis techniques, Int. J. Civ. Eng. Technol., 9 (2018) 1395–1403.

[34] M. H. Al-Helaly, I. A. Alwan, and A. N. Al-Hameedawi, Assessing land cover for Bahar Al-Najaf using maximum likelihood (ML) and artificial neural network (ANN) algorithms, J. Phys. Conf. Ser., 1973 (2021) 012190. https://doi.org/10.1088/1742-6596/1973/1/012190

[35] A. N. M. Al-Hameedawi, Comparison between Saaty's approach and Alonso and Lamata's approach in site selection process," IOP Conf. Ser. Mater. Sci. Eng., 737 (2020) 012217. https://doi.org/10.1088/1757-899X/737/1/012217

[36] S. H. Hasan, A. N. M. Al-Hameedawi, and H. S. Ismael, Supervised Classification Model Using Google Earth Engine Development Environment for Wasit Governorate, IOP Conf. Ser. Earth Environ. Sci., 961 (2022) 012051. https://doi.org/10.1088/1755-1315/961/1/012051

[37] M. S. Ozigis, J. D. Kaduk, and C. H. Jarvis, Mapping terrestrial oil spill impact using machine learning random forest and Landsat 8 OLI imagery: A case site within the Niger Delta region of Nigeria, Environ. Sci. Pollut. Res., 26 (2019) 3621–3635. https://doi.org/10.1007/s11356-018-3824-y

[38] M. S. Ozigis, J. D. Kaduk, C. H. Jarvis, P. da Conceição Bispo, and H. Balzter, Detection of oil pollution impacts on vegetation using multifrequency SAR, multispectral images with fuzzy forest and random forest methods, Environ. Pollut., 256 (2020) 113360. https://doi.org/10.1016/j.envpol.2019.113360

[39] V. Vapnik, The nature of statistical learning theory. Springer science & business media, 1999.

[40] V.Cherkassky, The nature of statistical learning theory~, IEEE Trans. Neural Networks, 8 (1997) 1564. https://doi.org/10.1109/tnn.1997.641482

[41] P. K. Srivastava, D. Han, M. A. Rico-Ramirez, M. Bray, and T. Islam, Selection of classification techniques for land use/land cover change investigation, Adv. Sp. Res., 50 (2012) 1250–1265. https://doi.org/10.1016/j.asr.2012.06.032

[42] S. Talukdar et al., Land-use land-cover classification by machine learning classifiers for satellite observations-A review, Remote Sens., 12 (2020) 1135. https://doi.org/10.3390/rs12071135

[43] P.Mather and B. Tso, Classification methods for remotely sensed data. CRC press, 2016. https://doi.org/10.1201/9781420090741

[44] H. Keshtkar, W. Voigt, and E. Alizadeh, Land-cover classification and analysis of change using machine-learning classifiers and multi-temporal remote sensing imagery, Arab. J. Geosci., 10 (2017) 1–15. https://doi.org/10.1007/s12517-017-2899-y

[45] R. G. Congalton and K. Green, Assessing the accuracy of remotely sensed data: principles and practices. CRC press, 2019.

[46] A. S. J. Al-Saedi, Z. M. Kadhum, and B. S. Jasim, Land Use and Land Cover Analysis Using Geomatics Techniques in Amara City, Ecol. Eng, 9 (2023) 161–169. https://doi.org/10.12912/27197050/173211

[47] B. Gworek and J. Rateńska, Mercury migration in pattern air-soil-plant, Ochr. Środowiska i Zasobów Nat., 41 (2009) 614-623.